ISSN 1063-7737, Astronomy Letters, 2021, Vol. 47, No. 2, pp. 117–122. © Pleiades Publishing, Inc., 2021.
Russian Text © The Author(s), 2021, published in Pis'ma v Astronomicheskii Zhurnal, 2021, Vol. 47, No. 2, pp. 138–144.

On the Relationship between the Magnetic Field of a Low-Latitude Coronal Hole and Its Area

Z. S. Akhtemov[1*] and Yu. T. Tsap[1]

[1] *Crimean Astrophysical Observatory, Russian Academy of Sciences, Nauchny, 298409 Russia*

Received August 24, 2020; revised November 17, 2020; accepted November 26, 2020

Abstract—Based on the data obtained with the CHIMERA algorithm, we consider the evolution of a long-lived low-latitude coronal hole during its central meridian passage over the period from February 15, 2012, to October 14, 2012. The correlation coefficient between the photospheric magnetic field strength of the coronal hole and its area in nine Carrington rotations is $R = -0.55$. It differs noticeably from $R = -0.82$ given in Heinemann et al. The results suggest a significant dependence of the area of coronal holes on the method of determining their boundaries. This can have a noticeable effect both on the prediction of geomagnetic activity and on the understanding of the nature of solar phenomena related to these structures.

DOI: 10.1134/S1063773721010011

Keywords: *Sun, coronal holes, magnetic fields.*

INTRODUCTION

Coronal holes (CHs) are large-scale ($\sim 10^{20}$ cm^2) structures of the solar corona that differ from the surrounding quiet regions by an open magnetic field configuration and by reduced plasma density and temperature (see, e.g., Cranmer 2009). CHs are observed in the soft X-ray and extreme ultraviolet ranges on the solar disk as dark structures, while in He I 10 830 Å images they have an enhanced brightness. The interest in CHs stems primarily from the fact that they are the source of the fast solar wind (Cranmer 2002, 2009; Akhtemov and Tsap 2018), which has a significant effect not only on the near-Earth space, but also on the Earth. In particular, the so-called corotating interaction regions being formed in the solar corona can give rise to weak and moderate geomagnetic storms (Yermolaev et al. 2018).

In recent years the questions related to the CH magnetic field have aroused great interest (Heinemann et al. 2018; Hofmeister et al. 2017, 2019). This is primarily explained by the fact that so far there are no clear views of how the solar wind accelerates (Cranmer 2002, 2009). Its speed is believed to be closely related not only to the CH area (Nolte et al. 1976; Shugai et al. 2009; Rotter et al. 2012; Akiyama et al. 2013; Akhtemov and Tsap 2018), but also to the CH magnetic field strength. In particular, a correlation with the averaged CH magnetic field and the rate of decrease in its strength with height characterized by super-radial flux-tube expansion has been found (Wang and Sheeley 1990; Kojima et al. 2007; Wang 2010; Fujiki et al. 2015).

Relatively recently, having studied the evolution of one of the long-lived low-latitude CHs for eight months in 2012 based on data from the Atmospheric Imaging Assembly (AIA) and Helioseismic and Magnetic Imager (HMI) instruments onboard the Solar Dynamics Observatory (SDO) satellite, Heinemann et al. (2018) concluded that there exists a high correlation (a Pearson correlation coefficient $R = -0.82$) between the CH area and averaged photospheric magnetic field. This conclusion somewhat contradicts the earlier statistical results for different CHs (see, e.g., Bilenko and Tavastsherna 2017). Meanwhile, the estimate obtained is of great phenomenological importance, because it suggests that the magnetic field variations inside CHs determine their evolution.

Heinemann et al. (2018) extracted the CH boundaries based on the adopted intensity threshold relative to the median intensity for the solar disk in the AIA/SDO 193 Å channel. Meanwhile, determining the CH boundaries is a rather complex and ambiguous problem due to the inhomogeneity of the atmosphere and often a low CH contrast compared to the neighboring quiet solar regions. The fact that the CH areas can differ considerably in the solar disk images at different wavelengths being formed approximately at the same height in the transition region and the lower corona also plays a significant role (Garton et al. 2018). The determination of the CH boundaries is also complicated by the superposition of brighter

*E-mail: azis@craocrimea.ru

and darker structures, such as streamers, jets, coronal loops, and filaments, on low-latitude CHs.

Thus, although the technique for determining the CH boundaries in Heinemann et al. (2018) follows from the analysis of the highest-contrast ultraviolet AIA/SDO images of CHs, it nevertheless seems too simplified. The approach proposed in Garton et al. (2018) looks more justified. The method of automated CH detection and identification with the Coronal Hole Identification via Multi-thermal Emission Recognition Algorithm (CHIMERA) developed by these authors allows the CH boundary contours to be determined using three AIA/SDO 171, 193, and 211 Å channels in the extreme ultraviolet emission of iron ions to which the typical plasma temperatures of 6.3×10^5, 1.6×10^6, and 2.0×10^6 K correspond (Lemen et al. 2012). We would especially like to emphasize that the degree of openness of the magnetic field configuration up to 2.5 $R_\odot$, according to the Potential Field Source Surface Model (PFSS) using HMI/SDO magnetograms in the photospheric Fe I 6173 Å line as the input data, is also taken into account in the algorithm.

The goal of this paper is to study the relationship between the area and magnetic field of a long-lived low-latitude CH when its center of mass crosses the zero (central) meridian, then to compare the results obtained with the corresponding relationship from Heinemann et al. (2018), and finally to discuss the consequences of our analysis and to propose a possible interpretation.

RELATIONSHIP BETWEEN THE CH AREA AND MAGNETIC FIELD FROM THE CHIMERA DATA

As in Heinemann et al. (2018), we chose the period from February 15, 2012, to October 14, 2012 (Carrington rotations CR2121–CR2129) corresponding to the second growth phase of the 24th solar cycle. At this time a long-lived, isolated, and relatively compact CH was observed on the solar disk at low latitudes (Fig. 1), which allowed the projection effects to be minimized. We determined the averaged area $A_{\rm CH}$ and longitudinal magnetic field $B_{\rm CH}$ when the CH center of mass passed through the central meridian on February 15, 2012; March 13, 2012; April 9, 2012; May 6, 2012; June 3, 2012; June 30, 2012; July 26, 2012; August 22, 2012; September 18, 2012; and October 14, 2012. However, in contrast to Heinemann et al. (2018), who developed their own algorithm following from the analysis of AIA solar disk images in the highest-contrast 193 Å line and the adopted threshold value of 35% of the median solar disk intensity, we invoked CHIMERA, the software algorithm that is described in Garton et al. (2018) and is in free access (https://github.com/TCDSolar/CHIMERA) for practical use. As the input data for the chosen time interval we used four FITS (Flexible Image Transport System) files from the SDO archive: an HMI magnetogram and three AIA images in the 171, 193, and 211 Å channels. Using the code, we constructed solar disk images with CH boundaries and created a text file containing information about the coordinates of the center of mass (geometrical center), the area, and the mean longitudinal magnetic field strength at the CH base at the photospheric level. During each passage of the CH center of mass through the central meridian we constructed five CH images within ±7° in longitude, corresponding to approximately ±15 h. Using several CH images allowed us to reduce the geometrical distortions and to increase the accuracy of measurements. The data obtained in this way were then averaged and were used by us as the quantities characterizing the CH at the time of its passage through the central meridian. This approach may be deemed justified if the CH parameters do not change significantly over this time interval. Note that Heinemann et al. (2018) also found the radial magnetic field of the identified CH as a result of the data averaging, but within ±18 h of the passage of the CH center of mass through the central meridian. During this period of observations the CH contours from the CHIMERA data remained within ±50° in latitude and ±30° in longitude.

Following Heinemann et al. (2018), we characterized the correlation between the CH area and averaged magnetic field by a linear Pearson correlation coefficient R defined with standard notation in a well-known way (see, e.g., Aivazyan 1968; Gmurman 1972):

$$R = \frac{\sum_{i=1}^{n}(X_i - \bar{X})(Y_i - \bar{Y})}{\sqrt{\sum_{i=1}^{n}(X_i - \bar{X})^2 \sum_{i=1}^{n}(Y_i - \bar{Y})^2}}. \quad (1)$$

Given the small sample size n, to estimate the confidence interval CI, we used Fisher's Z-transformation (Aivazyan 1968)

$$Z = \operatorname{arctanh} R = 0.5 \ln\left(\frac{1+R}{1-R}\right).$$

In this case, the lower (Z_L) and upper (Z_U) boundaries are, respectively, (Aivazyan 1968)

$$Z_L = \operatorname{artanh} R - \frac{t_\gamma}{n-3} - \frac{R}{2(n-1)}, \quad (2)$$

$$Z_U = \operatorname{artanh} R + \frac{t_\gamma}{n-3} - \frac{R}{2(n-1)}.$$

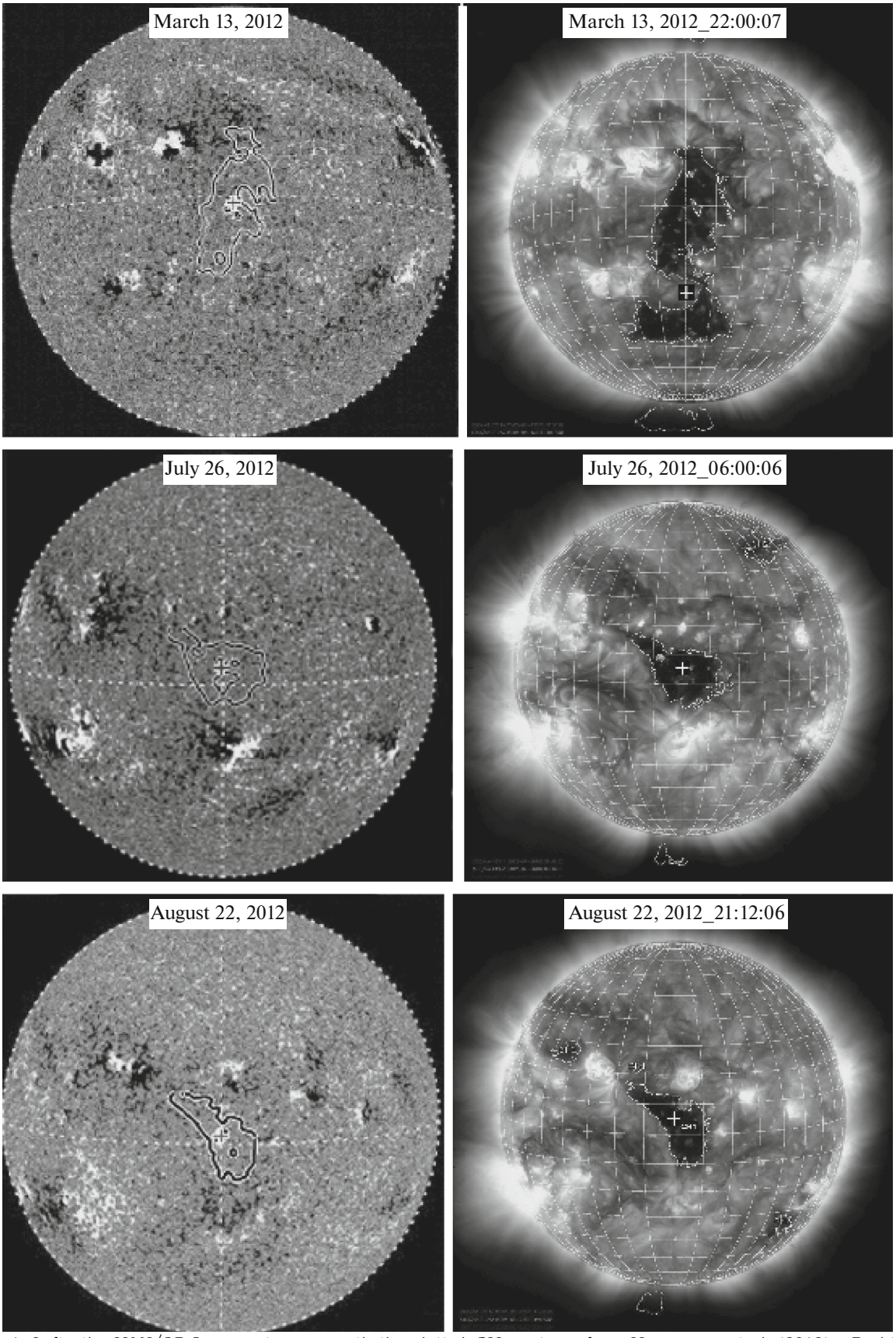

Fig. 1. Left: the HMI/SDO magnetograms with the plotted CH contours from Heinemann et al. (2018). Right: the synthesized AIA/SDO images in the 171, 193, and 211 Å channels after the determination of the CH boundaries with PFSS, according to CHIMERA (Garton et al. 2018).

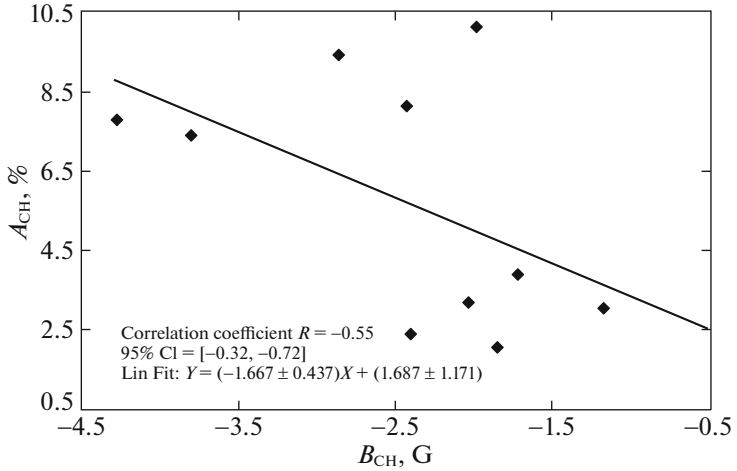

Fig. 2. Relationship between the averaged CH area A_{CH} and longitudinal magnetic field B_{CH} from the CHIMERA data. The area A_{CH} is expressed in percent of the solar disk area.

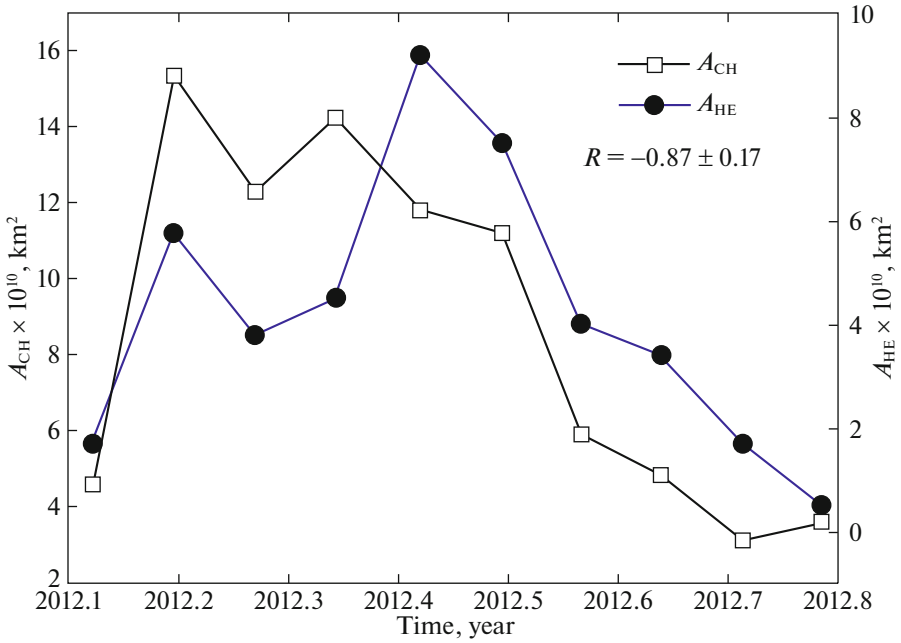

Fig. 3. Time dependence of the averaged CH areas as derived by Heinemann et al. (2018), A_{HE}, and with CHIMERA, A_{CH}, over the period from February 15, 2012, to October 14, 2012 (CR2121-CR2129) during the CH passage through the central meridian.

For a given confidence probability γ the quantile t_γ was calculated from the equation $\Phi(t_\gamma) = \gamma/2$, where the Laplace function

$$\Phi(t_\gamma) = \frac{1}{\sqrt{2\pi}} \int_0^{t_\gamma} e^{-x^2/2} dx.$$

Then, as follows from (2), the correlation coefficient must lie within the range

$$\tanh Z_L < R < \tanh Z_U, \qquad (3)$$

where the hyperbolic tangent

$$\tanh Z = \frac{\exp(2Z) - 1}{\exp(2Z) + 1}.$$

Figure 2 shows the relationship between the averaged area A_{CH} and longitudinal magnetic field B_{CH} of a low-latitude CH derived by us with CHIMERA for ten points obtained by averaging the measurements near the central meridian. The regression line and the regression equation are also displayed here. According to Eq. (1), the linear Pearson correlation coefficient is $R = -0.55$. Since $t_\gamma =$

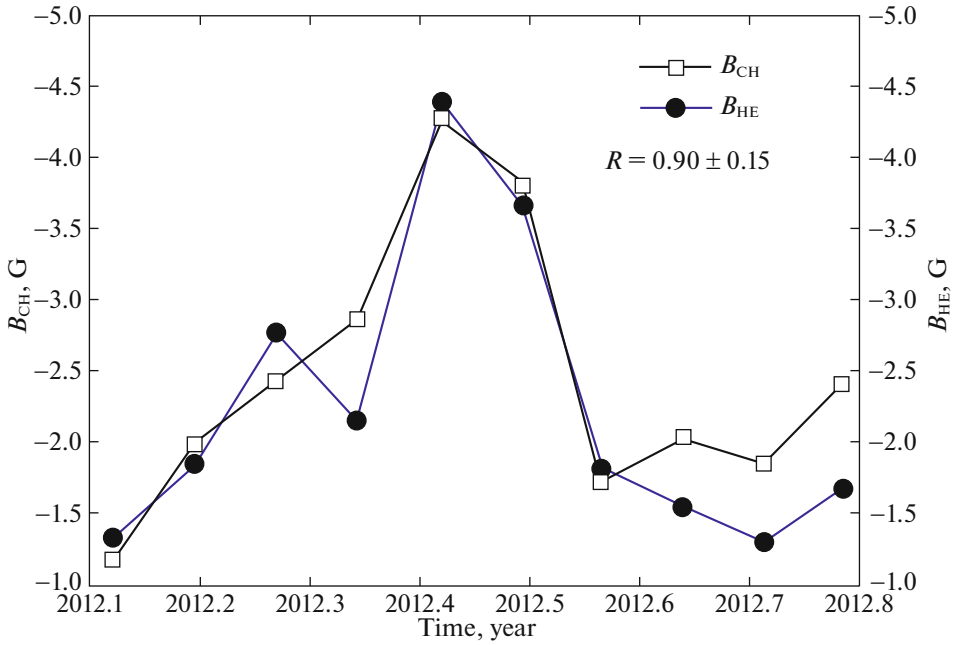

Fig. 4. Time dependence of the averaged CH magnetic field strengths as derived by Heinemann et al. (2018), B_{HE}, and with CHIMERA, B_{CH}, over the same period as that in Fig. 3 during the CH passage through the central meridian.

1.96 for the confidence probability $\gamma = 0.95$ (Gmurman 1972), in this case, given (2) and (3), the confidence interval is $CI = [-0.32, -0.72]$. These estimates suggest a rather weak correlation between the CH area and mean magnetic field strength, which somewhat contradicts the results from Heinemann et al. (2018), according to which $R = -0.82$ and $CI = [-0.36, -0.97]$ at $\gamma = 0.95$, i.e., the correlation between the quantities under study is high.

It seems that the revealed discrepancy in the results is primarily explained by a strong dependence of the CH boundaries on the technique of their determination. In Fig. 1 (upper panel) it can be seen how the boundaries vary noticeably and the difference in the areas derived by Heinemann et al. (2018), A_{HE}, and with CHIMERA, A_{CH}, can reach 30% (Fig. 3), although the correlation coefficient is $R = -0.87 \pm 0.17$. Meanwhile, the averaged CH magnetic field strengths have a smaller scatter. This is confirmed by the results of our calculations (Fig. 4), according to which $R = 0.90 \pm 0.15$ for the averaged magnetic fields B_{HE} and B_{CH}. Note that the above estimates of R are consistent with the previously made assumption (Akhtemov et al. 2020) about a stronger dependence of the CH magnetic flux on their area than on the field strength.

DISCUSSION AND CONCLUSIONS

Based on the AIA/SDO and HMI/SDO satellite data obtained with CHIMERA for the identified CH, we, in contrast to Heinemann et al. (2018), failed to find a high correlation between the CH area variations and magnetic field strength at the photospheric level during the CH passage through the central meridian over the period from February 15, 2012, to October 14, 2012. In our view, even if the small sample size is taken into account, this is explained by the fact that the techniques for determining the CH boundaries in Heinemann et al. (2018) and Garton et al. (2018) differ noticeably. In the former case a method based on 193 Å images was used for the CH identification on the solar disk, while in the latter case multiwavelength ultraviolet observations and, what is particularly important, HMI/SDO magnetograms were used. It can be assumed that one of the possible causes of so significant differences is related to the fine CH structure and the superposition of various magnetic structures near the CH boundary. In our view, the conclusion reached by Heinemann et al. (2018) about the existence of a high correlation between the CH area and magnetic field strength should be revised. This also suggests the necessity of developing unified approaches to the problem of determining the CH boundaries, because otherwise it will be difficult to avoid significant errors in predicting space weather and properly interpreting the CH-related phenomena.

The presented results suggest that the magnetic field strength variations inside CHs have no decisive effect on the evolution of their area. This conclusion is confirmed, in particular, by the results from Saqri et al. (2020) based on AIA/SDO observations, suggesting that the ultraviolet plasma density and

temperature in the CH under study are virtually independent of its area. Since the magnetic field is closely related to coronal plasma heating, this is indicative of minor magnetic field variations at coronal heights. Hence, given the dominant contribution to the CH magnetic flux from small-scale elements (Hofmeister et al. 2017, 2019), it can be assumed that the CH contours must be closely related to the processes near the boundaries. As a result of interchange reconnection (Shelke and Pande 1984; Kong et al. 2018), reconnection between open and closed magnetic fluxes can occur due to the evolution of global and local characteristics in the outer CH region accompanied by a change in the field configuration and, accordingly, the CH areas.

In contrast to sunspots, in which the magnetic field strength increases with their area (Bray and Loughhead 1967; Nagovitsyn et al. 2017; Obridko and Nagovitsyn 2017), we failed to find the corresponding pattern for CHs. This suggests a different origin of these structures probably related to a significant difference in their scales and formation heights.

ACKNOWLEDGMENTS

We are grateful to the referees for their careful reading of the paper and their useful remarks, which contributed significantly to its improvement. This work was supported in part by the Russian Foundation for Basic Research (project no. 20-52-26006) and the Ministry of Education and Science (NIR no. 0831-2019-0006).

REFERENCES

1. S. A. Aivazyan, *Statistical Study of Dependences* (Metallurgiya, Moscow, 1968) [in Russian].
2. Z. S. Akhtemov and Yu. T. Tsap, Geomagn. Aeron. **58**, 1149 (2018).
3. Z. S. Akhtemov, Y. T. Tsap, and V. I. Haneychuk, Astrophysics **63**, 399 (2020).
4. S. Akiyama, N. Gopalswamy, S. Yashiro, and P. Makela, Publ. Astron. Soc. Jpn. **65**, S15 (2013).
5. I. A. Bilenko and K. S. Tavastsherna, Geomagn. Aeron. **57**, 803 (2017).
6. R. J. Bray and R. E. Loughhead, *Sunspots* (Chapman and Hall, London, 1964).
7. S. R. Cranmer, Space Sci. Rev. **101**, 229 (2002).
8. S. R. Cranmer, Liv. Rev. Solar Phys. **6**, 3 (2009).
9. K. Fujiki, M. Tokumaru, T. Iju, K. Hakamada, and M. Kojima, Solar Phys. **290**, 2491 (2015).
10. T. M. Garton, P. T. Gallagher, and S. A. Murray, J. Space Weather Space Climate **8**, 02 (2018).
11. V. S. Gmurman, *Probability Theory and Mathematical Statistics* (Vysshaya Shkola, Moscow, 1972) [in Russian].
12. S. G. Heinemann, S. J. Hofmeister, A. M. Veronig, and M. Temmer, Astrophys. J. **863**, 29 (2018).
13. S. J. Hofmeister, A. Veronig, M. A. Reiss, M. Temmer, S. Vennerstrom, B. Vrsnak, and B. Heber, Astrophys. J. **835**, 268 (2017).
14. S. J. Hofmeister, D. Utz, S. G. Heinemann, A. Veronig, and M. Temmer, Astron. Astrophys. **629**, A22 (2019).
15. M. Kojima, M. Tokumaru, K. Fujiki, H. Itoh, T. Murakami, and K. Hakamada, in *New Solar Physics with Solar-B Mission,* Ed. by K. Shibata, S. Nagata, and T. Sakurai, ASP Conf. Ser. **369**, 549 (2009).
16. D. F. Kong, G. M. Pan, X. L. Yan, J. C. Wang, and Q. L. Li, Astrophys. J. **863**, L22 (2018).
17. J. R. Lemen, A. M. Title, D. J. Akin, P. F. Boerner, C. Chou, J. F. Drake, D. W. Duncan, Ch. G. Edwards, et al., Solar Phys. **275**, 17 (2012).
18. Y. A. Nagovitsyn, A. A. Pevtsov, and A. A. Osipova, Astron. Nachr. **338**, 26 (2017).
19. J. T. Nolte, A. S. Krieger, A. F. Timothy, R. E. Gold, E. C. Roelof, G. Vaiana, A. J. Lazarus, and J. D. Sullivan, Solar Phys. **46**, 303 (1976).
20. V. N. Obridko and Yu. A. Nagovitsyn, *Solar Activity, Cyclicity, and Prediction Methods* (VVM, St. Petersburg, 2017) [in Russian].
21. T. Rotter, A. M. Veronig, M. Temmer, and B. Vrsnak, Solar Phys. **281**, 793 (2012).
22. J. Saqri, A. M. Veronig, S. G. Heinemann, S. J. Hofmeister, M. Temmer, K. Dissauer, and Y. Su, Solar Phys. **295**, 6 (2020).
23. R. N. Shelke and M. C. Pande, Bull. Astron. Soc. India **12**, 404 (1984).
24. Yu. S. Shugai, I. S. Veselovsky, and L. D. Trichtchenko, Geomagn. Aeron. **49**, 415 (2009).
25. Y.-M. Wang, Astrophys. J. **715**, L121 (2010)
26. Y.-M. Wang and N. R. Sheeley, Astrophys. J. **355**, 726 (1990).
27. Yu. I. Yermolaev, I. G. Lodkina, N. S. Nikolaeva, M. Yu. Yermolaev, M. O. Riazantseva, and L. S. Rakhmanova, J. Atmos. Sol.-Terr. Phys. **180**, 52 (2018).

Translated by V. Astakhov